 doi: 10.1111/j.1365-246X.2004.02253.x

Further evidence for low intensity of the geomagnetic field during the early Cretaceous time: using the modified Shaw method and microwave technique

Yongxin Pan,[1] Mimi. J. Hill,[2] Rixiang Zhu[1] and John Shaw[2]

[1] *Laboratory of Palaeomagnetism, Institute of Geology and Geophysics, Chinese Academy of Sciences, Beijing* 100101*, China.*
[2] *Geomagnetism Laboratory, Department of Earth and Ocean Science, University of Liverpool, Liverpool* L69 7ZE*, UK. E-mail: mimi@liv.ac.uk*

Accepted 2004 February 2. Received 2004 January 15; in original form 2002 November 28

SUMMARY

We report new absolute palaeointensity estimates using basalts from northeastern China (K/Ar age, 125–120 Ma) using the modified Shaw method in conjunction with the microwave technique. Samples for the palaeointensity experiments were selected mainly based on their good reversibility of thermomagnetic curves and single primary magnetization characteristics. Using the modified Shaw method, 28 out of 45 measured samples from 10 cooling units give a virtual dipole moment of $(3.1 \pm 1.0) \times 10^{22}$ Am^2, and the microwave technique using 14 acceptable determinations (out of 20 measured) give an average value of $(2.9 \pm 0.9) \times 10^{22}$ Am^2. Results using both the modified Shaw method and the microwave technique demonstrate that the geomagnetic field strength recorded by these lavas was low. This is in agreement with previous results of the same time interval obtained by the Thellier method with partial thermal remanence (p-TRM) checks. The fact that different techniques give qualitatively compatible low palaeointensity results provides greater confidence that the weak field features seen just prior to the Cretaceous normal superchron (CNS) are the result of the actual field recorded by the basalts as opposed to artefacts of the method/analysis. This study also demonstrates that the microwave technique can be used for very old basalts.

Key words: absolute palaeointensity, basalt, China, microwave palaeointensity technique, modified Shaw method.

1 INTRODUCTION

A knowledge of the past behaviour of the geomagnetic field is important if we are to understand the processes in the Earth's deep interior, e.g. outer-core dynamics and core–mantle coupling, in a time dimension that other geophysical measurements lack (Courtillot & Besse 1987; Pal & Roberts 1988; Merrill & McFadden 1990; Prévot *et al.* 1990; Larson & Olson 1991; Glatzmaier *et al.* 1999; Valet 2003). In the past decade, much effort has been made to obtain absolute palaeointensity data through geological time using various techniques (e.g. Valet *et al.* 1996; Laj *et al.* 1997; Goguitchaichvili *et al.* 1999; Riisager *et al.* 1999; Goguitchaichvili *et al.* 2000; Thomas *et al.* 2000; Tarduno *et al.* 2001; Zhu *et al.* 2001; Goguitchaichvili *et al.* 2002a; Hill *et al.* 2002; Riisager *et al.* 2002; Shi *et al.* 2002). However, despite these recent efforts to obtain palaeointensity data, there is a general lack of such data and so a detailed understanding of how the long-term field strength has changed is not well known. Using what data is currently available, a number of proposals have been made. For example Biggin & Thomas (2003a) analysed the existing palaeointensity database and proposed a generic geodynamic model to explain the relationship between global geodynamic processes and the long-term changes in field intensity. Heller *et al.* (2003) found that there is a bimodal distribution of field intensity over the past 320 Myr and tentatively suggest that the geodynamo could have two polarity states.

One of the major debates regarding long-term field strength variations is associated with the existence of a Mesozoic dipole low (MDL) as proposed by Prévot *et al.* (1990), during which the dipole strength was found to be only one third of the Cenozoic value. Juarez *et al.* (1998) and Selkin & Tauxe (2000) argued using only data obtained from the Thellier method with partial thermal remanence (p-TRM) checks, that the MDL was instead part of a general feature of an intensity low that existed from 300 to 0.3 Ma. The validity of the MDL has also been questioned by Goguitchaichvili *et al.* (2002b) following an analysis of the 160–5 Ma part of the palaeointensity record. Several palaeointensity investigations have indicated that the intensity during the Cretaceous normal superchron (CNS) could be similar to or much higher than the present field (e.g. Tarduno *et al.* 2001; Tauxe & Staudigel 2003). Several statistical analyses of the palaeointensity database do however support the existence of an MDL (e.g. Perrin & Scherbakov 1997; Heller *et al.* 2002; Thomas & Biggin 2003). The intensity prior to the CNS is also of great interest but has similar contradiction, for example, Goguitchaichvili *et al.* (2002a) recently obtained a mean value of $(7.2 \pm 2.3) \times 10^{22}$ Am^2 from early Cretaceous Paraná flood basalts (133–132 Ma), which is 92 per cent of the present geomagnetic field, suggesting that at that time palaeointensity might be comparable or even much higher than recent field intensity and that the MDL may not be a real feature. This is clearly inconsistent with the claim of low values during early Cretaceous time found by other earlier studies (e.g. Pick & Tauxe 1993; Zhu *et al.* 2001). At present, with the limited data available, it is not possible to resolve these differences thus it is essential that more reliable palaeointensity data from the Mesozoic time is obtained before the intriguing differences between results can be resolved and the validity of the MDL and other long-term variations of intensity can be ascertained.

Extensively distributed volcanic sequences in northeastern China from Jurassic to Cretaceous age offer a very attractive opportunity for palaeomagnetic investigations. Early Cretaceous volcanic rocks have been studied using the modified Thellier method (Zhu *et al.* 2001, 2003). In this paper we report further palaeointensity estimates from these basalts but this time using the modified Shaw and the new microwave methods. The study provides further evidence that a weak geomagnetic field existed prior to the CNS.

2 GEOLOGICAL SETTING, SAMPLES AND PREVIOUS PALAEOMAGNETIC STUDIES

Large-scale lithospheric extension and volcanism occurred in northeastern China from the late Jurassic to early Cretaceous (Chen *et al.* 1997). The early Cretaceous Yixian Formation, lying uncomformably above the middle Jurassic Tuchengzi Formation, is mainly composed of andesite basalt, tuffs, breccias and lake sediments, which are well exposed in the Fuxin–Beipiao–Yixian basin (Fig. 1). Palaeobiologists have recently focused attention on the diverse fossil assemblages from the lake sediment intervals, in particular early bird fauna and feathered dinosaurs. Elemental studies of volcanic rocks indicated that basalts were derived from partial melting of lithosphere mantle (Li *et al.* 2001). Previous radiometric age determinations using K/Ar and $^{40}Ar/^{39}Ar$ methods give *ca* 135 to 120 Ma for the major eruptive cycle (Chen *et al.* 1997; Zhu *et al.* 2002).

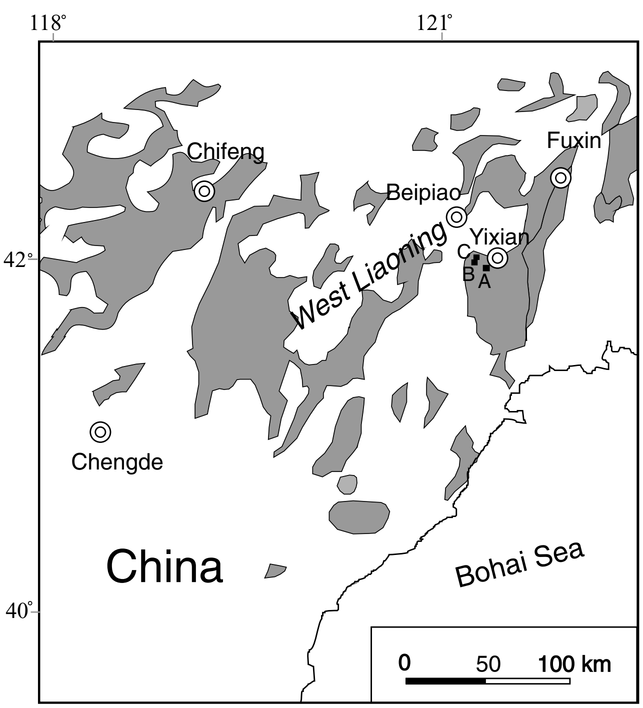

Figure 1. Map showing the distribution of the early Cretaceous strata in northeastern China and the three sampling sites used in this study, A - Zhuanchengzi (ZCZ), B - Sihetun (SHT) and C - Huangbanjiegou (HBJG).

The basalt samples used in this study were collected from three sections named the Zhuanchengzi (ZCZ, 121.1°E/41.5°N), Sihetun (SHT, 120.8°E/41.8°N) and Huangbanjiegou (HBJG, 120.8°E, 41.9°N) sections (Fig. 1) in two field sessions in 1999. The ZCZ section is composed of 20 lava flows that erupted in a very short time period approximately 120 Ma (K–Ar age). Previous palaeomagnetic studies by Zhu *et al.* (2001) show that the lava flows (with a thickness ranging from 3 to 11 m) are reversely magnetized with a mean direction of $D/I = 174.9°/-60.1°(\alpha_{95} = 2.3)$. The SHT section, located 20–25 km south of Beipiao city, consists of the upper basalts, middle fossil-bearing lake sediments and the lower lava flows. The lake sediments are normally magnetized and have been attributed to the M3n polarity chron (Pan *et al.* 2001). The lava flows (with a thickness ranging from 2 to 12 m) have been dated to give an age of 133–124 Myr. It has been observed that the upper and the lower basalts were reversely and normally magnetized with mean palaeodirections of $D/I = 175.9°/-60°(\alpha_{95} = 6.4)$ and $D/I = 5.4°/58.7°(\alpha_{95} = 2.4)$, respectively (Zhu *et al.* 2003). The HBJG section is approximately 2 km north of the SHT section. It consists of six basaltic-andesite lava flows with a total thickness of 25 m, which is overlaid by a light-greyish fossil-bearing lake sediment interval. Bubble horizons and lithologic colours were used for lava flow division in the field. Samples were collected using a portable gasoline-powered drill. All cores were vertically distributed inside a cooling unit and orientated *in situ* using a magnetic compass and/or a sun compass. Absolute palaeointensity determinations using the modified Thellier method have been conducted on the ZCZ and SHT sections previously (Zhu *et al.* 2001, 2003). The samples that were remaining were used for this study. The K–Ar method was used for age determination: see Zhu *et al.* (2001) for a detailed description of the method. Ages for all the cooling units studied are reported in Table 1.

3 ROCK-MAGNETIC EXPERIMENTS, DEMAGNETIZATION OF NATURAL REMANENT MAGNETIZATION (NRM) AND SAMPLE SELECTION

Rock-magnetic studies were conducted to identify the magnetic minerals that carry the NRM as well as to determine thermal

Table 1. Radiometric ages and palaeodirectional results.

Site	Age ± 2.δ (Ma)	H(m)	n/N	Dec.	Inc.	α_{95}	*P* lat.	*P* long.
Zhuanchengzi (ZCZ)								
Z01	120.9 ±2.3^a	11.0	4/4	172.2	−61.9	7.1	−84.0	229.4
Z12	120.7 ±2.3^b	7.0	3/4	170.1	−61.4	1.7	−82.6	222.3
Z17	120.5 ±2.3^a	8.0	4/4	164.9	−60.6	1.4	−78.7	216.5
Z20	121.0 ±2.4^a	5.0	3/4	173.0	−57.0	6.3	−83.3	177.5
Sihetun (SHT)								
S03	124.4 ±2.4^b	7.1	4/5	177.4	−58.5	7.3	−86.7	159.0
S05	124.6 ±2.5^c	9.0	5/5	4.7	56.9	6.9	84.4	259.3
S06	124.8 ±2.3^c	12.0	5/5	3.0	59.6	8.9	87.4	240.9
S08	124.9 ±2.4^b	2.7	3/5	348.9	60.0	5.7	81.6	28.3
Huangbanjiegou (HBJG)								
H03		5.4	4/5	0.3	57	4.9	85.7	297.6
H04	125.4 ±3.3^d	3.8	4/6	9.3	56.4	6.5	81.3	242.3

H, thickness of lava flow; n/N, number of samples used in the calculation and total number demagnetized; Dec./Inc., declination and inclination; *P* lat./*P* long., latitude and longitude of VGPs. (a) After Zhu *et al.* (2001), (b) after Zhu *et al.* (2002), (c) after Zhu *et al.* (2003) and (d) this study.

stability. Strong field (in a steady field of 800 mT) thermomagnetic analyses were performed on a Magnetic Measurements Variable Field Translation Balance (MMVFTB) at the University of Liverpool. Heating and cooling were in air atmosphere with rates of the order of 8–10 °C min^{-1}. The results of 67 representative samples from the three sections allow discrimination of three major types of behaviour.

Type A, observed for 62 per cent of the samples, is characterized by a regular decay of the induced magnetization from room temperature to 450 °C, followed by a rapid decrease to a Curie temperature (Tc), which varies between 550–580 °C (Fig. 2a). The cooling curves are reversible following the heating curves. These samples contain a single ferromagnetic phase, probably a low Ti titanomagnetite.

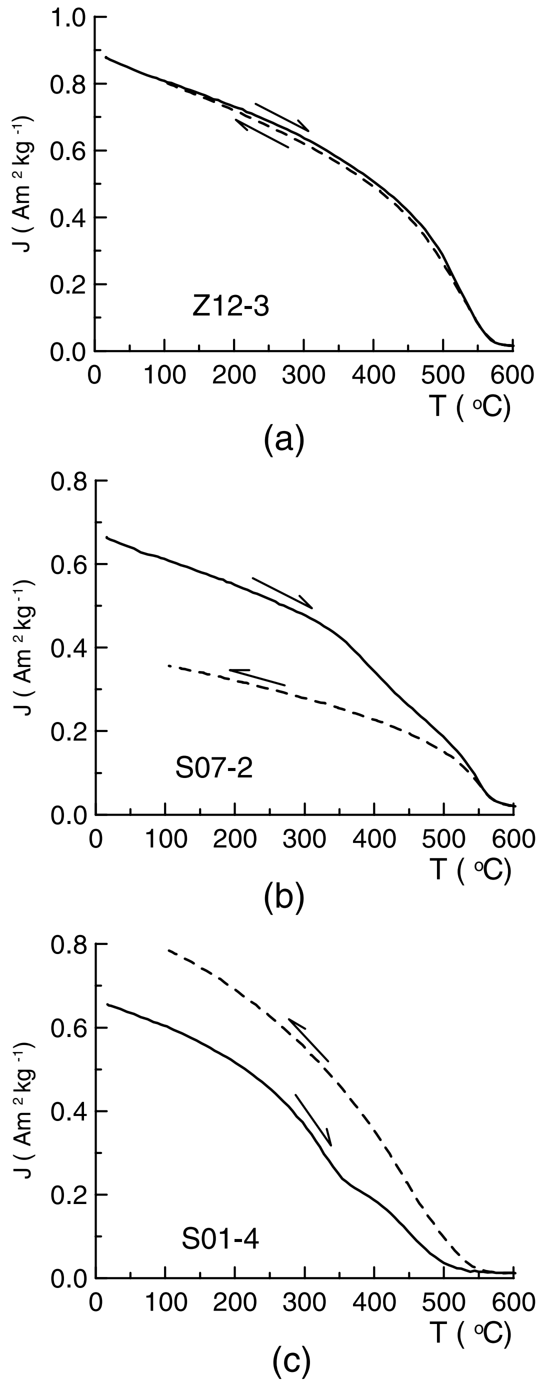

Figure 2. Typical thermomagnetic curves. Samples were heated at a rate of ∼8–10 °C min^{-1}in a steady field of 800 mT in air atmosphere. Solid (dashed) lines correspond to heating (cooling) curves.

Type B, observed in 30 per cent of the measured samples, is characterized by heating curves with two Curie points. The first magnetization drop is between 350 and 450 °C and the second one close to 570 °C (Fig. 2b). The cooling curve shows a single Curie point close to the second high temperature on the heating curve and lies far below the heating curve. This behaviour may be attributed to the breakdown of maghemite into weaker haematite with increasing temperature.

Type C, observed in 8 per cent of the measured samples, is also characterized by two Curie points, the first occurs between 350 to 400 °C, while the second is close to 510 to 550 °C (Fig. 2c). However, in this case the cooling curve usually lies above the heating curve. The increase in magnetization could reflect exsolution of low Ti titanomagnetite occurring at high temperature (Ade-Hall *et al.* 1971).

The reversibility of heating and cooling curves of Type A indicates their good thermal stability and suitability for palaeointensity experiments. Samples of types B and C were excluded from palaeointensity experiments, because the magnetic mineral alteration by heating as indicated by the thermomagnetic curves may lead to false palaeointensity estimations. This is less of a concern for the microwave palaeointensity technique where alteration is minimized (e.g. Hill & Shaw 1999), however, to maximize reliable palaeointensity estimations, only type A samples (single phase) were selected for all palaeointensity experiments. In total, 75 samples from five cooling units of the ZCZ section (Nos Z01, Z12, Z11, Z17 and Z20), four of the SHT section (Nos S03, S05, S06 and S08) and two of the HBJG section (Nos H03 and H04), were chosen based on the thermomagnetic curves.

Saturated isothermal remanence acquisition, back-field demagnetization and hysteresis properties of at least two representative samples from each chosen lava flow were also measured on the MMVFTB. Most of the measured samples (total 27 samples) fall into the pseudo-single-domain (PSD) range (Day *et al.* 1977) or a mixture of single-domain (SD) and multidomain (MD) grains (Dunlop 2002), but close to a coarser MD region on a Day plot (Fig. 3). We discarded four samples of lavas Nos S05, 06 and H03 as a

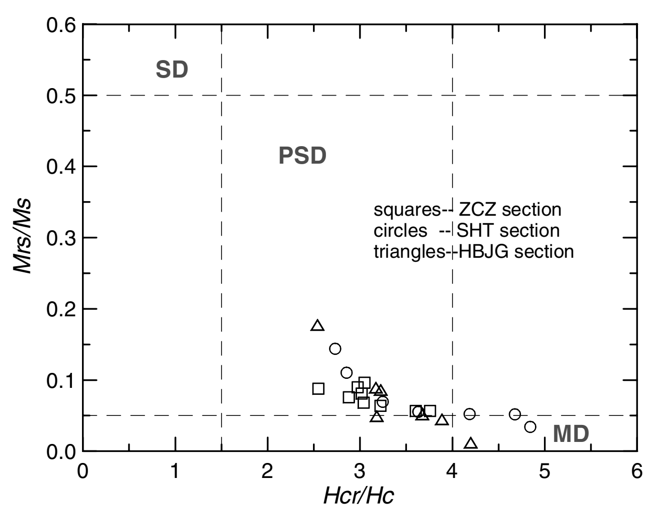

Figure 3. Day plot for samples used in palaeointensity experiments. Squares, circles and triangles stand for ZCZ, SHT and HBJG sections, respectively.

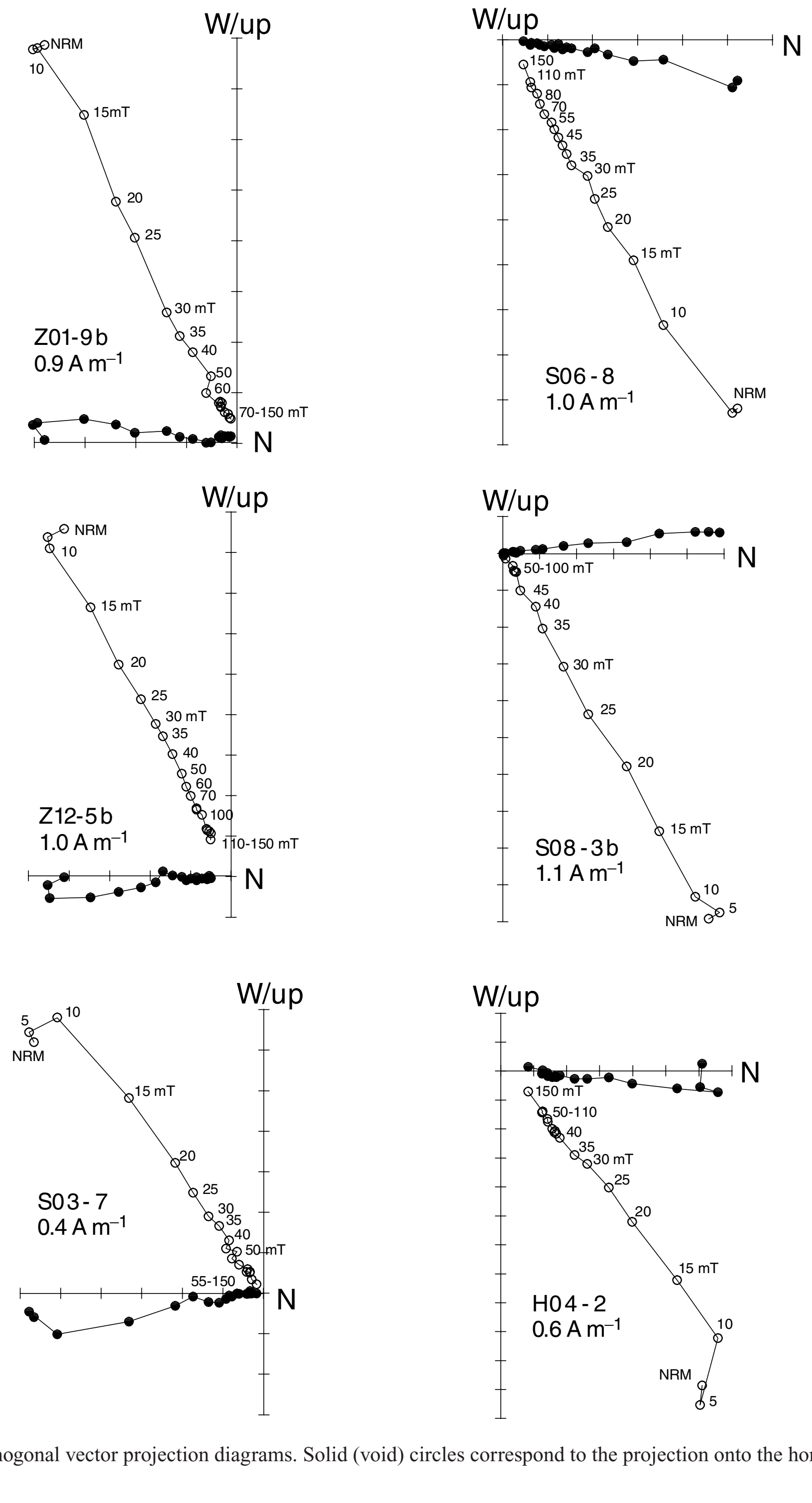

Figure 4. Representative orthogonal vector projection diagrams. Solid (void) circles correspond to the projection onto the horizontal (vertical) planes.

result of their MD grain characteristics. The observation that samples reach 90 per cent of their saturation isothermal remanent magnetization (SIRM) by 200–300 mT and remanence coercivity (Hcr) in 15–30 mT indicate that titanomagnetite is the main remanence carrier.

Stepwise alternating field (a.f.) demagnetization of NRM was performed on a tumbling a.f. demagnetizer, as part of the palaeointensity experiments using the Shaw method. Seventeen–twenty steps were used to an available maximum peak field of 150 mT. Fields at 10–15 mT clean a small viscous magnetization and a single characteristic remanence (ChRM) component heading towards the origin was isolated from higher coercivity intervals (Fig. 4). For each sample, the ChRM was determined by means of a least-squares method (Kirschvink 1980). For each flow, the direction of individual specimens was averaged and statistical parameters calculated assuming a Fisherian distribution. Directional results are presented in Table 1. The mean direction for five reversed cooling units is $D/I = 171.6^\circ/-59.9^\circ (\alpha_{95} = 2.9)$, nearly antiparallel to that for the five normal ones of $D/I = 1.5^\circ/58.2^\circ (\alpha_{95} = 4.1)$. These results are consistent with previous directional results obtained using systematic thermal demagnetization by Zhu *et al.* (2001) and Zhu *et al.* (2003). The difference in the mean declinations could be the result of secular variation indicating episodic eruption of the lavas. As palaeointensity determination requires the successful isolation of the primary component of magnetization, six samples that have either a large viscous component or ChRM directions that deviate from the origin were discarded in later palaeointensity experiments. Finally, in total 65 samples were selected for palaeointensity experiments (45 for the Shaw technique and 20 for the microwave technique).

4 PALAEOINTENSITY DETERMINATIONS

4.1 Modified Shaw method

The Shaw method (Shaw 1974) relies on the fact that a change in thermal remanence (TRM) coercivity spectra necessarily means that there is a change in ARM (Anhysteretic Remanent Magnetization) coercivity spectra. If a part of the ARM_2 coercivity after heating is the same as the ARM_1 coercivity before heating then that part of the coercivity spectra is unaltered and the NRM/TRM ratio can be determined from the unaltered part of the coercivity spectra.

Palaeointensity experiments were performed on 45 selected samples using the following procedure:

(i) The NRM was stepwise a.f. demagnetized with increasing values of the peak a.f. up to 100–150 mT in 17–20 steps.

(ii) Samples were given an anhysteretic remanence in a maximum peak a.f. of 150 mT and a 0.1 mT direct field (ARM_1). The ARM_1 was then stepwise a.f. demagnetized and measured as in step (i).

(iii) Samples were given a TRM by heating to 600 °C, holding for 30 min and cooling in a constant field of (50 ±0.1) μT. The TRM was subsequently a.f. demagnetized and measured as in step (i).

(iv) Samples were given an ARM_2 as in step (ii). This ARM_2 was a.f. demagnetized as in step (i). To minimize the influence of residual remanence inherited from previous procedures, demagnetization with a peak a.f. of 150 mT was performed between two successive procedures.

Mineral alteration may occur during TRM acquisition in step (iii), which requires a single heating to above the Curie point (600 °C), which may lead to significant TRM capacity changes. The modified Shaw method with ARM correction, i.e. using ratios of anhysteretic remanent magnetization given before the TRM step (ARM_1) and after (ARM_2), has been assumed to be a powerful approach to correct such TRM capacity changes (Rolph & Shaw 1985). It is noted that the sample selections in this study based on thermomagnetic

Table 2. Palaeointensity results determined by Shaw method.

Site	Sample	*P*	mT	*n*	*f*	*r*	F_a (μT)	N	$F_m \pm$ s.d.(μT)
Z01	01-9b	1.1	25–120	12	0.47	0.991	28.2	3	29.7 ± 2.7
	01-11b	−1.5	35–70	5	0.29	0.991	32.8		
	01–13	−1.1	20–50	5	0.58	0.983	28.1		
Z12	12-2	−6.6	25–70	5	0.22	0.995	23.1	2	25.7
	12-5b	1.6	20–70	7	0.42	0.995	28.3		
Z17	17-2	−7.2	20–80	8	0.40	0.989	15.9	2	16.7
	17-7	−8.0	20–50	5	0.20	0.991	17.5		
Z20	20-2	0.1	25–60	5	0.29	0.984	11.6	2	14.8
	20-4b	−0.3	20–70	10	0.45	0.988	17.9		
S03	03-1	−6.7	20–80	8	0.27	0.986	13.5	3	13.3 ± 1.1
	03-2	5.6	25–55	6	0.19	0.991	14.2		
	03-7	−5.8	25–150	11	0.35	0.983	12.1		
S05	05-2	−3.3	20–45	6	0.19	0.981	15.6	4	15.4 ± 2.7
	05-5	2.7	15–55	5	0.29	0.994	14.0		
	05-7b	0.3	20–70	10	0.28	0.998	19.1		
	05-9	−5.9	15–70	10	0.32	0.982	12.9		
S06	06-1	−6.3	20–60	9	0.37	0.995	25.1	3	22.0 ± 3.4
	06-6	−5.8	10–70	12	0.69	0.999	22.5		
	06-8	1.4	20–70	10	0.41	0.997	18.3		
S08	08-2	4.6	20–80	12	0.78	0.999	16.1	3	19.9 ± 4.8
	08-3b	6.9	15–70	11	0.72	0.999	18.4		
	08-4	3.8	30–100	12	0.40	0.997	25.3		
H03	03-1	−8.7	15–50	8	0.26	0.991	14.7	2	15.1
	03-5	−9.3	15–80	12	0.61	0.996	15.5		
H04	04-2b	0.9	15–60	10	0.32	0.982	13.2	4	11.6 ± 1.4
	04-3b	2.0	15–60	10	0.29	0.983	12.3		
	04-4	2.1	15–60	8	0.30	0.986	10.9		
	04-7	2.7	15–80	12	0.27	0.990	10.1		
Mean							18.1 ± 6.2		18.8 ± 6.0

P is the alteration parameter (for definition see text); *n* is the number of data points; *f* is the percentage fraction of NRM used in the palaeointensity determination; *r* is the linear correlation coefficient of the best-fitting straight line; F_a is evaluated ancient field intensity in μT; *N* is the number of determinations used to calculate the flow mean; $F_m \pm$ s.d. is the lava flow mean value with the standard deviation; mean F_a is the mean and standard deviation of all intensity estimates; mean $F_m \pm$ s.d is the overall mean and standard deviation for accepted flow means (all except Z20; see text for further explanation).

properties help contribute to obtaining acceptable determinations. For most samples, the changes in low field magnetic susceptibility values measured before and after step (iii) were small, also suggesting limited magnetic mineral transformations occurred in the laboratory heating during the TRM acquisition procedure.

Pan *et al.* (2002) proposed to identify significant alteration as a result of heating, e.g. transformation of magnetite into haematite, by an alteration parameter P and also the necessity for the linearity between TRM and ARM_2. The P value has been defined (Pan *et al.* 2003) as the difference in remanence remaining after peak demagnetization of the NRM and TRM, i.e.

$$P = [res\,(\mathrm{TRM})/ini(\mathrm{TRM}) - res\,(\mathrm{NRM})/ini(\mathrm{NRM})] \times 100 \text{ per cent}$$

where *res* is the residual left after demagnetization and *ini* is the initial value. When significant viscous magnetization is present, the initial value of the NRM is taken to be the magnetization remaining once the ChRM has first been isolated. Correspondingly the

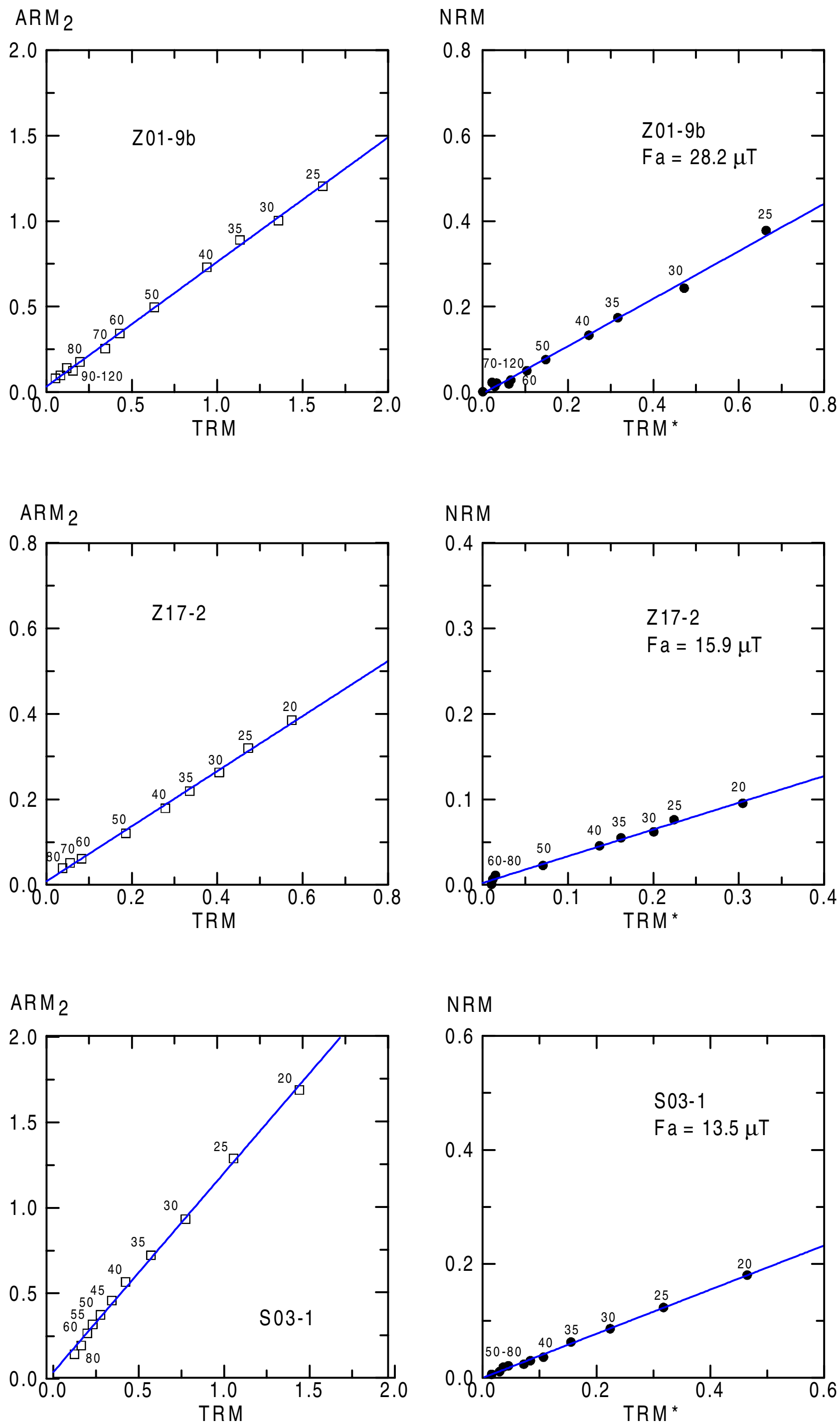

Figure 5. Representative results from the modified Shaw method. Left panel: TRM–ARM_2 plots; right panel: TRM*–NRM plots. TRM* = TRM × (ARM_1/ARM_2). Remanence in units: 10^{-3} Am^2 kg^{-1}. Fa is the evaluated palaeointensity. Labelled peak demagentization field is in mT.

initial TRM is taken as the remanence remaining after the same peak-field demagnetization that was used to isolate the ChRM. Twelve samples were rejected either because of non-linear sections on a TRM–ARM_2plot or because P values were greater than 10 per cent.

As to the remaining 33 samples, each TRM was corrected by multiplying by the corresponding ratio of (ARM_1/ARM_2) as proposed by Rolph & Shaw (1985), i.e.

$$TRM^* = TRM \times (ARM_1/ARM_2).$$

The slope of the linear interval of NRM/TRM* is calculated and the palaeointensity obtained. We accepted palaeointensity estimates if the following criteria were met:

(i) A primary component of NRM heading towards the origin that confines to the mean flow direction is present.

(ii) A recognized linearity of the TRM–ARM_2 plot and P value of less than 10 per cent.

(iii) The linear portion of NRM–TRM* contains not less than five points ($N \geq 5$) and not less than 15 per cent of the original

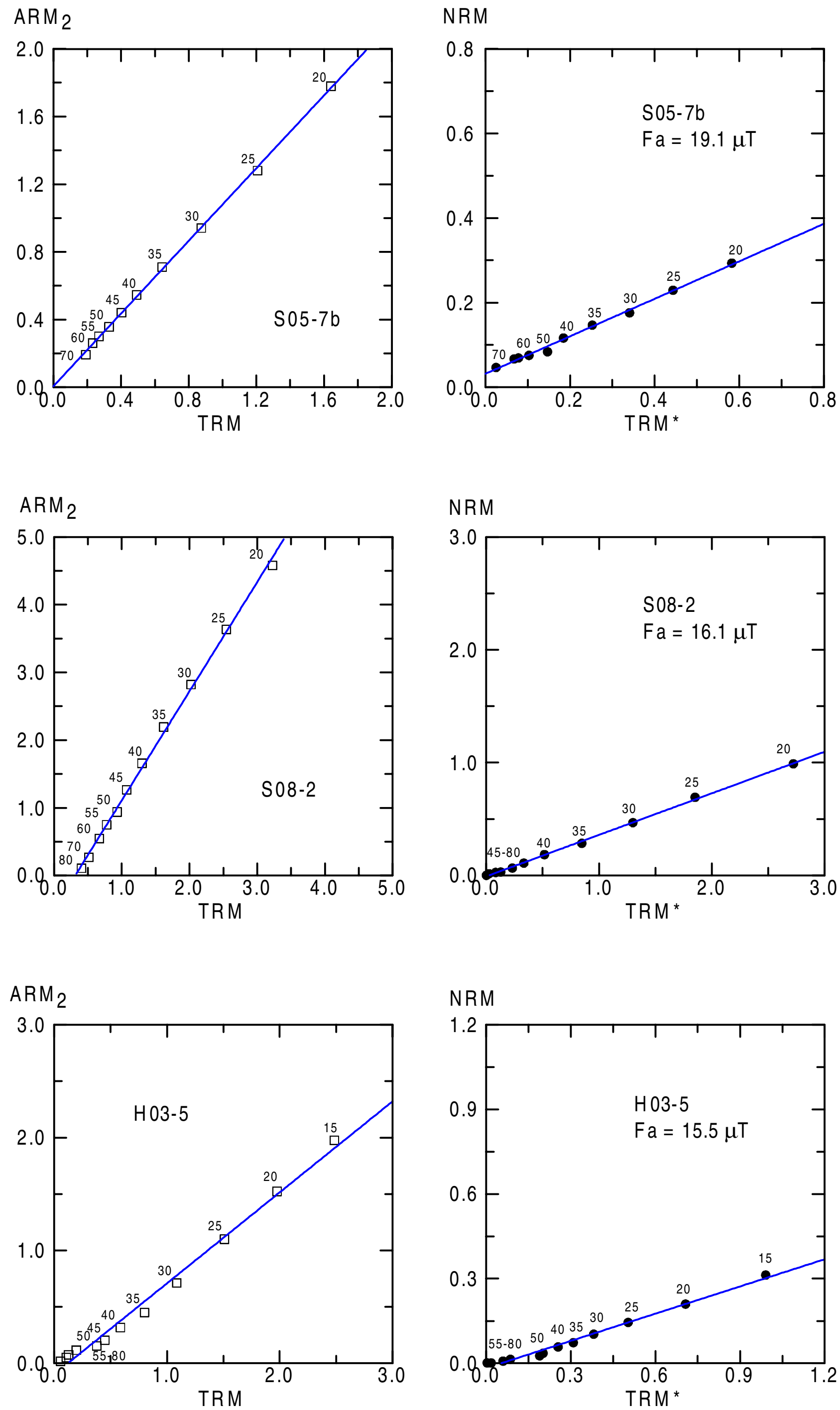

Figure 5. (*Continued.*)

NRM ($f \geq 0.15$) is used, similar to criteria of Yamamoto *et al.* (2003).

A total of 28 samples yielded palaeointensity estimations, see Table 2. Typical coercivity diagrams are presented in Figs 5(a) and (b). A further acceptance criteria is within flow self-consistency where the maximum acceptable standard deviation for a mean cooling unit is taken as 25 per cent (Selkin & Tauxe 2000). This study is limited by only a small number of samples being available from each lava flow, so for a number of flows there are only two estimates per flow. This means a flow mean standard deviation cannot be taken. It is noted that the two samples from flow Z20 differ by 35 per cent and are therefore not self-consistent.

The mean palaeointensity for all 28 samples is 18.1 ± 6.2 μT. Excluding flow Z20, the mean intensity for nine flows is 18.8 ± 6.0 μT. The ZCZ (excluding Z20), SHT and HBJG sections have average intensity values of 24.0 ± 6.7, 17.7 ± 4.0 and 13.4 ± 2.5 μT, respectively.

4.2 Microwave technique

20 5-millimetre diameter core samples were taken from 2.5 cm cores from seven cooling units (Nos Z01, Z11, Z12, Z20, S08, H03 and H04) from the three sections. The cooling unit Z11 was not included in the Shaw method study (as a result of limited sample availability) but was part of the Thellier study of Zhu *et al.* (2001). The samples were subjected to microwave palaeointensity analysis using the 8.2 GHz microwave system at the University of Liverpool. The microwave palaeointensity technique, described in detail by Hill & Shaw (1999), is a variant of the stepwise Thellier method (Kono & Ueno 1977). By using direct microwave excitation of the magnetic grains instead of conventional heating, the microwave technique can produce a thermoremanent magnetization without significantly heating the bulk sample, thus avoiding thermal alteration (Walton *et al.* 1993; Shaw *et al.* 1996; Hill & Shaw 2000). The microwave thermoremanence (T_MRM) is induced perpendicular to the direction of the NRM. Once the primary component of magnetization has been reached, the laboratory field is applied in a direction perpendicular to the NRM and then remains on for the rest of the experiment. The magnitude is set to be approximately the same as the ancient field (15, 20 or 30 μT in this study). Microwave power applied for 10 s at each step is the equivalent of temperature in conventional experiments and is increased incrementally until the sample has been completely remagnetized and the magnetization is in the direction of the applied field (or the maximum power of 200 W has been reached). The vector sum of the NRM and T_MRM components can be decomposed by software so that NRM remaining can be plotted against T_MRM gained, as in conventional Thellier experiments. Ideally, the data points result in a straight line with a gradient equal to the ratio of the natural to laboratory field strength. Checks are in place to ensure that the total vector of magnetization is in the NRM–T_MRM plane and if not these data points are discarded.

The microwave intensity results are shown in Table 3 . The acceptance criteria used are similar to those used in the previous Thellier studies (Zhu *et al.* 2001, 2003). The linear portion of the NRM–T_MRM plot must contain not less than five points ($n \geq 5$) and not less than 30 per cent of the original NRM ($f \geq 0.30$). The ratio of the standard error of the best fitting line to the slope of the same line must be less than 0.1 ($\beta \leq 0.1$) and the linear regression coefficient of the line must be greater than 0.98 ($r > 0.98$). From the seven cooling units, 14 out of 20 samples gave acceptable palaeointensity estimates. The two samples from the SHT section failed to produce a palaeointensity estimate, as it was not possible to demagnetize the samples using the maximum microwave power available. Two failed samples both from flow H04 did not produce linear NRM–T_MRM plots and two samples one from Z20 and one from H04 were rejected as a result of low f factors. Representative NRM–T_MRM plots are shown in Fig. 6. Low field intensity values are obtained for all samples ranging from 10.3 to 27.2 μT. The mean of all 14 estimates is 17.4 ± 5.5 μ T. There is only one estimate per flow for Z20, H03 and H04. It is noted that the two estimates for Z17 are not self-consistent and that the standard deviation of the mean for Z11 is 35 per cent and therefore does not fulfill the self-consistency criteria. The mean from flows Z01 and Z12 (which have more than one estimate per flow and meet self-consistency criteria) is 21.2 μT.

Table 3. Palaeointensity results determined by the microwave technique.

Site	Sample	n	f	g	β	q	r	F_a (μT)	δ	N	F_m ± s.d. (μT)
Z01	01-2	12	0.75	0.83	0.0242	25.59	0.997	12.5	0.5	3	15.3 ± 2.5
	01-6	7	0.75	0.77	0.0172	33.40	0.999	17.2	0.5		
	01-11	12	0.85	0.80	0.0272	24.84	0.996	16.2	0.7		
Z11	11-10	9	0.71	0.75	0.0371	14.37	0.995	19.0	1.3	4	15.0 ± 5.3
	11-4	16	0.66	0.80	0.0195	26.84	0.997	10.5	0.4		
	11-5	10	0.75	0.82	0.0184	33.38	0.998	10.3	0.3		
	11-9	15	0.78	0.92	0.0258	27.73	0.995	20.1	0.7		
Z12	12-6	8	0.50	0.62	0.0401	7.75	0.995	27.0	3.5	2	27.1
	12-7	10	0.67	0.80	0.0233	22.94	0.997	27.2	1.2		
Z17	17-4	15	0.63	0.88	0.0282	19.54	0.995	22.9	1.2	2	19.1
	17-5	13	0.44	0.86	0.0393	9.50	0.991	15.3	1.6		
Z20	20-4	8	0.42	0.83	0.0341	10.18	0.996	15.1	1.5	1	
H03	03-6	8	0.30	0.83	0.0439	5.71	0.994	19.3	3.4	1	
H04	04-3	9	0.30	0.72	0.0486	4.50	0.992	11.5	2.5	1	
Mean									17.4 ±5.5		21.2

n is the number of data points; f, g, β ($= \sigma$b/b) and q are the quality factors as defined by Coe *et al.* (1978); r is the correlation coefficient of the best-fitting straight line; F_a is evaluated field intensity in μT; error, δ, is the level of uncertainty taking the error as $1/q \times F_a$; N is the number of determinations used to calculate the non-weighted flow mean (F_m); mean F_a is the mean and standard deviation of all intensity estimates; mean F_m ± s.d is the overall mean and standard deviation for accepted flow means (Z01 and Z12; see text for further explanation).

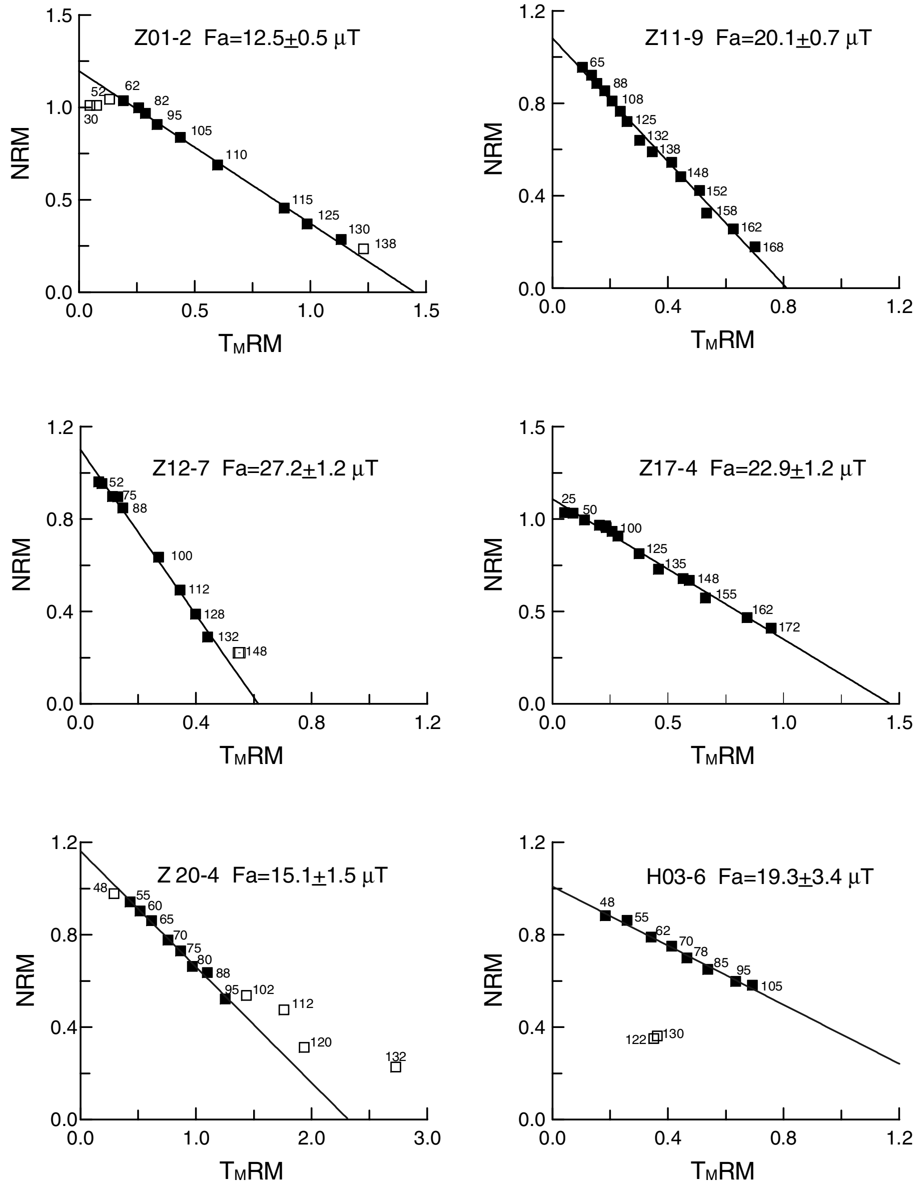

Figure 6. Representative results from the microwave intensity technique. Normalized NRM lost against T_MRM gained. The labels refer to applied power in watts.

5 DISCUSSIONS AND CONCLUSIONS

Fig. 7 presents the lava mean palaeointensity evaluated for each cooling unit from the three sections using the Shaw and microwave methods along with the previous Thellier results. All results have been included for comparative purposes. Before discussing the implications of these results and comparing them with the Thellier results, the following points should be noted:

(i) Palaeointensity experiments were conducted on 1–4 samples from each cooling unit and the recent study of Biggin *et al.* (2003) suggests that this is probably too few samples to obtain an accurate lava mean.

(ii) Among the five lavas studied by both methods in this study, only two sister samples were used as a result of limited sample availability. Six (five) sister samples from the previous Thellier study were studied using the Shaw (microwave) technique.

If we compare the Shaw and microwave results to previous published Thellier data, they are qualitatively comparable (Fig. 7). The significant feature of Fig. 7 is that estimates from all three methods indicate a weak magnetic field ranging from one third to one half the value of the present-day field at the same latitude, between 120–125 Ma.

Flow Z01, which has three samples investigated using each method, shows a spread of intensity estimates. The microwave method gives the lowest estimate of 15 μT and the Shaw method the highest of 30 μT with the Thellier result being in between. The microwave and Shaw methods are consistent with each other for flow Z20 but give estimates that are lower than the Thellier by 44 per cent, however there is only one microwave estimate and the two Shaw results are not self-consistent. Flow S05 again has the Shaw method results lower than the Thellier, this time by 36 per cent (there is no microwave data for this flow). Whilst there is not enough data to draw any significant conclusions from this, it is noted

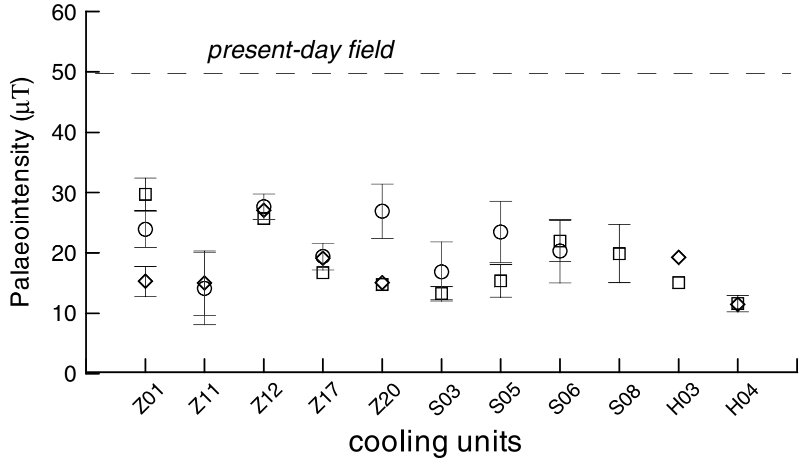

Figure 7. Comparisons of flow mean palaeointensity estimates with associated standard deviation. Where no error bars are present this indicates a mean value taken from only two samples per flow. The modified Shaw method (squares), microwave technique (diamonds) and comparison with the modified Thellier method (circles) by Zhu *et al.* (2001) and Zhu *et al.* (2003) additionally for each lava flow.

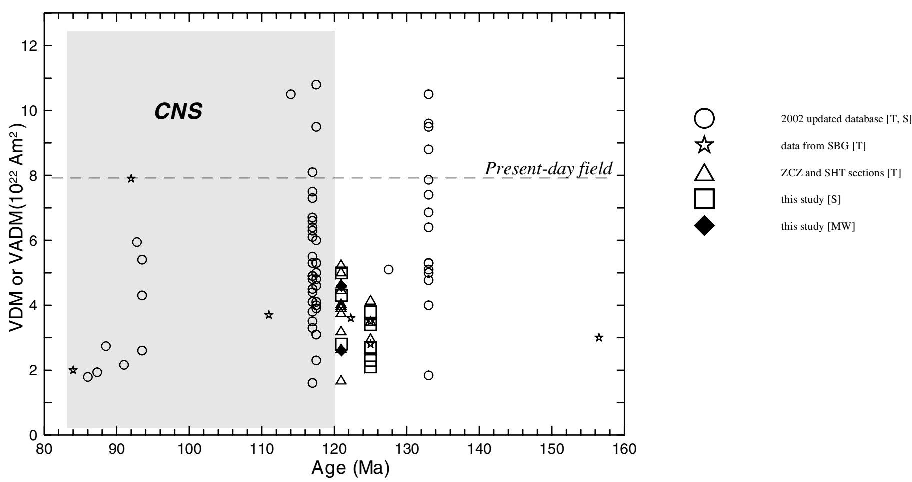

Figure 8. Comparison of results from this study with other published data from the 2002 updated database (using Thellier with p-TRM checks and Shaw method), Goguitchaichvili *et al.* (2002a) and Tanaka & Kono (2002), for 80–160 Ma time window (open circles). Data using SBG (Pick & Tauxe 1993; Juarez *et al.* 1998) open star, data of Zhu *et al.* (2001) and Zhu *et al.* (2003), open triangle, and results from this study using Shaw method (open square) and microwave method (closed diamond). The SBG data are VADMs. T, S and MW stand for Thellier method with p-TRM checks, Shaw method and microwave technique, respectively.

that three recent studies have observed incidences when seemingly reliable Thellier results produce over estimates of the palaeointensity (Calvo *et al.* 2002; Biggin & Thomas 2003b; Yamamoto *et al.* 2003).

Flow Z11 was investigated using the microwave (4 samples) and Thellier method (5 samples). Using both methods the standard deviation of the flow mean intensity is greater than 25 per cent (and both give similar flow mean intensities). The flow is not giving consistent intensity estimates and therefore may not be a reliable recorder of the magnetic field.

The intensity estimates determined by the modified Shaw method from 10 lava flows (total 28 samples) yield a mean virtual dipole moment (VDM) value of $(3.1 \pm 1.0) \times 10^{22}$ Am^2 and for the 9 self-consistent flows $(3.2 \pm 1.0) \times 10^{22}$ Am^2. The intensity values determined by the microwave technique from 7 lava flows (total 14 samples) yield a mean VDM value of $(2.9 \pm 0.9) \times 10^{22}$ Am^2 and for the 2 self-consistent flows (with more than one estimate) (3.6×10^{22}) Am^2. The Thellier method data for 8 flows (total 27 samples) have a mean VDM of $(3.7 \pm 1.1) \times 10^{22}$ Am^2 and excluding flow Z11 and S03 (as they aren't self-consistent) $(4.2 \pm 0.5) \times 10^{22}$ Am^2.

Our new estimations are consistent with results from other earlier studies at different locations for the same time interval as shown in Fig. 8. Pick & Tauxe (1993) determined palaeointensities using the Thellier method with p-TRM checks from submarine basalt glasses collected from the Caribbean sea with an age of 125 ±1 Myr. They calculated virtual axial dipole moments (VADMs) of $(2.8 \pm 0.7) \times 10^{22}$ Am^2 and $(3.5 \pm 1.9) \times 10^{22}$ Am^2 at holes 417D and 418A, respectively. The fact that comparable results were obtained from different geological materials also gives confidence that the data represents real geomagnetic field signals.

In summary, palaeointensity determinations using the modified Shaw method and the microwave technique from 11 lava flows spanning 125 to 120 Ma yield one third to one half the value of the present magnetic field of the Earth. These data are qualitatively consistent with earlier published estimations using the Thellier method with p-TRM checks. This study supports the existence of a weak dipole geomagnetic field prior to the CNS.

ACKNOWLEDGMENTS

The authors thank Daming Li for kind assistance in radiometric dating and D. N. Thomas and A. J. Biggin for very constructive comments and critical review of this manuscript. YXP is grateful to the Royal Society for supporting his stay in the University of Liverpool. MJH acknowledges the RAS for support to visit China during preparation of this manuscript. This work was supported by NSFC (grants 40325011 and 40221402), NERC (grant NER/A/S/2000/00676) and the Leverhulme Trust (grant F25BU).

REFERENCES

Ade-Hall, J.M., Palmer, H.C. & Hubbard, T.P., 1971. The magnetic and opaque petrological response of basalts to regional hydrothermal alteration, *Geophys. J. R. astr. Soc.,* **24,** 137–174.

Biggin, A.J. & Thomas, D.N., 2003a. Analysis of long-term variations in the geomagnetic poloidal field intensity and evaluation of their relationship with global geodynamics, *Geophys. J. Int.,* **152,** 392–415.

Biggin, A.J. & Thomas, D.N., 2003b. The application of acceptance criteria to results of Thellier palaeointensity experiments performed on samples with pseudo-single-domain-like characteristics, *Phys. Earth. planet. Int.,* **138,** 279–287.

Biggin, A.J., Böhnel, H.N. & Zúñiga, F.R., 2003. How many paleointensity determinations are required from a single lava flow to constitute a reliable average, *Geophys. Res. Lett.,* **30**(11), 1575, 2003GL017146.

Calvo, M., Prévot, M., Perrin, M. & Riisager, J., 2002. Investigating the reasons for the failure of palaeointensity experiments: a study on historical lava flows from MT. Etna (Italy), *Geophys. J. Int.,* **149,** 44–63.

Chen, W.J., Li, Q., Liang, H.D. & Xu, K., 1997. Geochronology of Mesozoic volcanic rocks and cyclicity of their volcanic activities in West Liaoning and its adjacent area, in *Volcanic Rocks in West Liaoning and its Adjacent Area: Chronology, Geochemistry and Tectonics,* pp. 168–201, eds Chen, Y.X. & Chen, W.J., Seismological Press, Beijing.

Coe, R.S., Gromme, C.S. & Mankinen, E.A., 1978. Geomagnetic paleointensities from radiocarbon-dated lava flows on Hawaii and the question of the Pacific nondipole low., *J. geophys. Res.,* **83,** 1740–1756.

Courtillot, V. & Besse, J., 1987. Magnetic field reversals, polar wander, and core-mantle coupling, *Science,* **237,** 1140–1147.

Day, R., Fuller, M.D. & Schmidt, V.A., 1977. Hysteresis properties of titanomagnetites: grain size and composition dependence., *Phys. Earth planet. Int.,* **13,** 260–266.

Dunlop, D.J., 2002. Theory and application of the Day plot (M_{rs}/M_s versus H_{cr}/H_c) 1. Theoretical curves and tests using titanomagnetite data, *J. geophys. Res.,* **107,** 10.1029/2001JB000486.

Glatzmaier, G.A., Coe, R.S. Hongre, L. & Roberts, P.H., 1999. The role of the Earth's mantle in controlling the frequency of geomagnetic reversals, *Nature,* **401,** 885–890.

Goguitchaichvili, A.T., Prevot, M.M., & Camps, P., 1999. No evidence for strong fields during the R3-N3 Icelandic geomagnetic reversal, *Earth planet. Sci. Lett.,* **167,** 15–34.

Goguitchaichvili, A., Chauvin, A., Roperch, P., Prevot, M., Aguirre, L. & Vergara, M., 2000. Palaeomagnetism of the Miocene Farellones formation (Chile), *Geophys. J. Int.,* **140,** 357–373.

Goguitchaichvili, A.T., Alva-Valdivia, L.M., Urrutia-Fucugauchi, J., Morales, J. & Lopes, O.F., 2002a. On the reliability of Mesozoic Dipole Low: New absolute paleointensity results from Parana Flood Basalts (Brazil), *Geophys. Res. Lett.,* **29(13),** 10.1029/2002GL015242.

Goguitchaichvili, A.T., Urrutia-Fucugauchi, J. & Alva-Valdiva, L., 2002b. Mesozoic dipole low: Myth or reality?, *EOS, Trans. Am. geophys. Un.,* **83(41),** 457–461.

Heller, R., Merrill, R.T. & McFadden, P.L., 2002. The variation of intensity of earth's magnetic field with time, *Phys. Earth planet. Int.,* **131,** 225–235.

Heller, R., Merrill, R.T. & McFadden, P.L., 2003. The two states of paleomagnetic field intensities for the past 320 million years, *Phys. Earth planet. Int.,* **135,** 211–223.

Hill, M. & Shaw, J., 1999. Palaeointensity results for historic lavas from MT. Etna using microwave demagnetization/remagnetization in a modified Thellier-type experiment, *Geophys. J. Int.,* **139,** 583–590.

Hill, M. & Shaw J., 2000. Magnetic field intensity study of the 1960 Kilauea lava flow, Hawaii, using the microwave paleointensity technique, *Geophys. J. Int.,* **142,** 487–504.

Hill, M.J., Gratton, M.N. & Shaw, J., 2002. Palaeomagnetic investigation of Tertiary lava from Barrington Tops, NSW, Australia, using thermal and microwave techniques, *Earth planet. Sci. Lett.,* **198,** 245–256.

Juarez, M.T., Tauxe, L., Gee, J.S. & Pick, T., 1998. The intensity of the Earth's magnetic field over the last 160 million years., *Nature,* **394,** 878–881.

Kirschvink, J.L., 1980. The least-square line and plane and analysis of paleomagnetic data., *Geophys. J. R. astr. Soc.***62,** 699–718.

Kono, M. & Ueno, N., 1977. Paleointensity determination by a modified Thellier method, *Phys. Earth planet. Int.,* **13,** 305–314.

Laj, C., Rais, A., Surmont, J., Gillot, P.-Y., Guillou, H., Kissel, C. & Zanella, E., 1997. Changes of the geomagnetic field vector obtained from lava sequences on the island of Vulcano (Aeolian Islands, Sicily)., *Phys. Earth planet. Int.,* **99,** 161–177.

Larson, R.L. & Olson, P., 1991. Mantle plumes control magnetic reversal frequency, *Earth planet. Sci. Lett.,* **107,** 437–447.

Li, W.P., Lu, F.X., Li, X.H., Zhou, Y.Q. & Zhang, D.G., 2001. The origin of early Cretaceous volcanic rocks of Yixian Formation and crust-mantle interaction in west Liaoning province, eastern China, *J. Mineral Petrol.,* **12**(4), 1–6 (in Chinese with English abstract).

Merrill, R.T. & McFadden, P.L., 1990. Paleomagnetism and the geodynamo, *Science,* **248,** 345–350.

Pal, P.C. & Roberts, P.H., 1988. Long-term polarity stability and strength of the geomagnetic diapole, *Nature,* **331,** 702–705.

Pan, Y.X., Zhu, R.X., Shaw J. & Zhou, Y.X., 2001. Magnetic polarity ages of the fossil-bearing strata at the Sihetun section, West Liaoning: A preliminary result, *Chinese Sci. Bull.,* **46**(17), 1473–1476.

Pan, Y.X., Shaw, J., Zhu, R.X. & Hill, M., 2002. Experimental reassessment of the Shaw paleointensity method by laboratory-induced thermal remanent magnetization, *J. geophy. Res.,* **107,** 10.1029/2001JB000620.

Pan, Y.X., Shaw, J., Zhu, R.X. & Hill, M., 2003. Reply to comment by Y. Yamamoto on 'Experimental reassessment of the Shaw paleointensity method by laboratory-induced thermal remanent magnetization', *J. geophys. Res.,* **108,** 10.1029/2002JB002355.

Perrin, M. & Scherbakov, V., 1997. Palaeointensity of the Earth's magnetic field for the past 400 Ma: evidence for a dipole structure during the Mesozoic, *J. Geomag. Geoelectr.,* **49,** 601–614.

Pick, T. & Tauxe, L., 1993. Geomagnetic palaeointensities during the Cretaceous normal superchron measured using submarine basaltic glass, *Nature,* **366,** 238–242.

Prévot, M., Derder, M.E., McWilliams, M. & Thompson, J., 1990. Intensity of the Earth's magnetic field: evidence for a Mesozoic dipole low., *Earth planet. Sci. Lett.,* **97,** 129–139.

Riisager, J., Perrin, M. & Rochette, P., 1999. Palaeointensity results from Ethiopian basalts: implications for the Oligocene geomagnetic field strength, *Geophys. J. Int.,* **138,** 590–596.

Riisager, P., Riisager, J., Abrahamsen, N. & Waagstein, R., 2002. Thellier paleointensity experiments on Faroes flood basalts: technical aspects and geomagnetic implications, *Phys. Earth planet. Int.,* **131,** 91–100.

Rolph, T.C. & Shaw, J., 1985. A new method of paleofield magnitude correction for the thermally altered samples and its application to Lower Carboniferous lavas, *Geophys. J. R. astr. Soc.,* **80,** 773–781.

Selkin, P. & Tauxe, L., 2000. Long-term variations in palaeointensity, *Phil. Trans. R. Soc. Lond.,* A., **358,** 1065–1088.

Shaw, J., 1974. A new method of determining the magnitude of the paleomagnetic field, Application to five historic lavas and five archaeological samples, *Geophys. J. R. astr. Soc.,* **39,** 133–141.

Shaw, J., Walton, D., Ang, S., Rolph, T.C. & Share, J.A., 1996. Microwave archaeointensity from Peruvian ceramics, *Geophys. J. Int.,* **124,** 241–244.

Shi, R.P., Zhu, R.X., Pan, Y.X., Shi, G.H. & Hoffman K.A., 2002. Palaeointensity study of Early Miocene lavas from Pingzhuang, Inner Mongolia, China, *Geophys. Res. Lett.,* **29**(21), 2026, 2002GL015990.

Tanaka, H. & Kono M., 2002. Paleointensities from a Cretaceous basalt platform in Inner Mongolia, northeastern China, *Phys. Earth planet. Int.,* **133,** 147–157.

Tarduno, J.A., Cottrell, R.D. & Smirnov, A.V., 2001. High geomagnetic intensity during the Mid-Cretaceous from Thellier analyses of single plagioclase crystals., *Science,* **291,** 1779–1783.

Tauxe, L. & Staudigel, H., 2003. Strength of the Geomagnetic Field in the Cretaceous Normal Superchron: New Data from Submarine Basaltic Glass of the Troodos Ophiolite, Abstract from, '*The Chapman Conference on Timescales of the Geomagnetic Field* ', University of Florida, Gainesville, American Geophysical Union.

Thomas, D.N. & Biggin, A.J., 2003. Does the Mesozoic dipole low really exist?, *EOS, Trans., Am. geophys. Un.,* **84**(11), 97 103–104.

Thomas, D.N., Biggin, A.J. & Schmidt, P.W., 2000. A palaeomagnetic study of Jurassic intrusive from southern New South Wales: further evidence for a pre-Cenozoic dipole low, *Geophys. J. Int.,* **140,** 621–635.

Valet, J.-P., 2003. Time variations in geomagnetic intensity, *Rev. Geophys.,* **41,** 1004, 10.1029/2001RG000104.

Valet, J.-P., Brassart, J., Le Meur, I., Soler, V., Quidelleur, X., Tric E. & Gillot, P.Y., 1996. Absolute paleointensity and magnetomineralogical changes, *J. geophys. Res.,* **101,** 25 029–25 044.

Walton, D., Share, J.A., Rolph T.C. & Shaw, J., 1993. Microwave magnetization, *Geophy. Res. Lett.,* **20,** 109–111.

Yamamoto, Y., Tsunakawa, H. & Shibuya, H., 2003. Palaeointensity study of the Hawaiian 1960 lava: implications for possible causes of erroneously high intensities, *Geophys. J. Int.,* **153,** 263–276.

Zhu, R.X., Pan, Y.X., Shaw, J., Li, D.M. & Li Q., 2001. Paleointensity just prior to the Cretaceous Normal Superchron, *Phys. Earth. planet. Int.,* **128,** 207–222.

Zhu, R.X., Shao, J.A., Pan, Y.X., Shi, R.P., Shi, G.H. & Li, D.M., 2002. Paleomagnetic data from Early Cretaceous volcanic rocks of West Liaoning: Evidence for intracontinental rotation, *Chinese Sci. Bull.,* **47**(21), 1832–1837.

Zhu, R.X., Hoffman, K.A., Pan, Y.X., Shi, R.P. & Li, D.M., 2003. Evidence for weak geomagnetic field intensity prior to the Cretaceous normal superchron, *Phys. Earth. planet. Int.,* **136,** 187–199.